

Finite-size particles, advection, and chaos: A collective phenomenon of intermittent bursting

Rene O. Medrano-T.,¹ Alessandro Moura,² Tamás Tél,³ Iberê L. Caldas,¹ and Celso Grebogi²

¹*Instituto de Física, Universidade de São Paulo, Caixa Postal 66318, 05315-970 São Paulo, Brazil*

²*College for Physical Sciences, King's College, University of Aberdeen, Aberdeen AB24 3UE, United Kingdom*

³*Lorand Eotvos University, Institute of Theoretical Physics, H-1518 Budapest, Hungary*

(Received 28 April 2008; published 12 November 2008; corrected 2 December 2008)

We consider finite-size particles colliding elastically, advected by a chaotic flow. The collisionless dynamics has a quasiperiodic attractor and particles are advected towards this attractor. We show in this work that the collisions have dramatic effects in the system's dynamics, giving rise to collective phenomena not found in the one-particle dynamics. In particular, the collisions induce a kind of instability, in which particles abruptly spread out from the vicinity of the attractor, reaching the neighborhood of a coexisting chaotic saddle, in an autoexcitable regime. This saddle, not present in the dynamics of a single particle, emerges due to the collective particle interaction. We argue that this phenomenon is general for advected, interacting particles in chaotic flows.

DOI: [10.1103/PhysRevE.78.056206](https://doi.org/10.1103/PhysRevE.78.056206)

PACS number(s): 05.45.-a, 47.52.+j

I. INTRODUCTION

The dynamics of systems with a great number of particles has been studied since the middle of the nineteenth century, when Maxwell published his ground-breaking work on the molecular velocity distribution of homogeneous gases. He realized that for that system, the details of the local dynamics are not important to understand the collective behavior of the system, which can be completely characterized by macroscopic quantities such as temperature, pressure, and volume. This extreme simplification is due to the homogeneity and isotropy of ideal gases. On the other hand, interacting systems often present complex dynamical structures that are important for the global behavior, which are not amenable to such simplifications. One of the most important examples is fluid motion, which commonly results in chaos in the motion of advected particles. Chaotic advection gives rise to intricate fractal structures in phase space, which have dramatic consequences for the global behavior of the system. The dynamics of noninteracting advected particles in chaotic flows has been extensively studied, and chaotic advection is a very active and current area of research.

Chaotic advection is found in both closed flows, where the motion is restricted to a finite volume, and in open flows, where fluid is constantly flowing through an interaction region from an upstream to a downstream direction. In the latter case, we have transient chaos, and the chaotic set is a nonattracting set of orbits with a fractal structure—a chaotic saddle. A closed flow may also have a chaotic saddle coexisting with a strange attractor. In either case the presence of chaotic saddles results in a very erratic and unpredictable transient motion by advected particles, which is related to its fractal geometry. Many important flow systems have been studied in terms of the transient advection dynamics, including chemical and biological collective process [1], chemical reactions [2,3], plankton blooming [4,5], and population dynamics [6]. For a review, see Ref. [7].

Most of the models for particle advection assume for simplicity the particles to be ideal tracers, that is, to have zero size and no inertia. Although the study of the motion of ideal

tracers yields valuable insights into the dynamics of advected particles, a better understanding of realistic systems requires that the finite size and inertia of the particles be considered. The main consequence of the inclusion of finite size and inertia is the appearance of Stokes' drag force, produced by the flow's viscosity, which introduces dissipation into the system. Due to the finite particle size, even in the case where the particles have the same density as the fluid, they do not follow the same trajectory as ideal tracers in time-dependent flows. As a result, these systems can exhibit attractors [8–10], for both bubbles (particles with lower density than the fluid) [11], and aerosols (particles with higher density than the fluid) [12], and other phenomena such as superpersistent chaotic transients under noise [13].

In the works mentioned in the previous paragraph, even though the finite size and nonvanishing inertia of real particles are considered, they are still considered to move independently, without interacting with each other. The study of single-particle phenomena is undoubtedly an important step in understanding the dynamics of many-particle systems in chaotic flows. However, this approach misses entirely the collective effects caused by interactions among the particles. A few recent studies have addressed collisions between particles in turbulent flows. For bubbles, collisions are enhanced in low-vorticity regions, a phenomenon referred to as a preferential concentration [14,15]. This can result in the appearance of organized patterns in space [16]. In flows, clusters may appear due to inelastic collisions among the particles [17]. In these works, however, the particles are considered to be ghost particles—the distance between two particles can be smaller than the sum of their radii, so that they are allowed to overlap with each other.

In this work we consider advected particles colliding in a time-dependent chaotic flow. The particles are solid spheres (they are not considered to be ghost particles), colliding elastically off each other. The dynamics of a single particle has a quasiperiodic global attractor. But, because of the collisions, they do not converge to this attractor. Our main result is the uncovering of the existence of a kind of instability due to the collective dynamics: the collisions induce the particles to burst out from the neighborhood of the single-particle quasi-

periodic attractor and to reach a coexisting chaotic saddle. This is a collective phenomenon not present in the collisionless dynamics and is a result of the inter-particle interaction due to the collisions. After reaching the chaotic saddle, the particles stay in its neighborhood for some time before returning to the neighbourhood of the quasiperiodic attractor, and then the cycle is repeated again. As a result, there is a striking pulslike oscillation in the spatial distribution of the particles. This instability is caused by the increasing rate of collisions among the particles as they approach the quasiperiodic attractor, and are squeezed into a low-dimensional set. This phenomenon has no counterpart in the collisionless system, and represents a feature arising from the collective dynamics due the collisions. One of the striking features of this phenomenon is that the chaotic saddle which is observed in the system's dynamics is not present in the collisionless dynamics; it is created by the interparticle interactions, and it mirrors the structure of a chaotic saddle present in the collisionless dynamics for a different parameter range.

Another interesting point revealed by the collisional dynamics is that the system behaves as an autoexcitable system. We show that this excitable behavior can be understood from the interplay between a quasiperiodic attractor present in the collisionless dynamics and the stable manifold of a coexisting chaotic saddle. Particles which reach the vicinity of the stable manifold of the chaotic saddle perform long, complex trajectories before returning to the vicinity of the quasiperiodic attractor.

II. THE MODEL

Although we expect our results to hold for a broad range of systems, we focus here on the dynamics of N particles of radius r which are much heavier than the fluid ($\rho_p \gg \rho_f$, where ρ_p and ρ_f are the particle and fluid densities, respectively); in other words, we consider aerosols. The particles are considered rigid and undeformable, thus the collisions are elastic and instantaneous. The particles are advected by a 2D incompressible flow, and are acted on by a gravitational field. To illustrate our results, we choose a simple 2D fluid velocity field with a time-smoothened alternating sinusoidal shear flow [10,18]

$$\begin{aligned} u_x(y,t) &= 0.5 \left[1 + \tanh\left(\frac{20 \sin(2\pi t)}{\pi}\right) \right] \sin(2\pi y), \\ u_y(x,t) &= 0.5 \left[1 - \tanh\left(\frac{20 \sin(2\pi t)}{\pi}\right) \right] \sin(2\pi x), \end{aligned} \quad (1)$$

where u_x and u_y are the fluid velocity components in the x and y directions, respectively. Equation (1) describes passive advection by a chaotic flow having a "mixed" phase space, presenting Kolmogorov-Arnold-Moser (KAM) islands as well as chaotic regions. This is a simple flow, amenable to numerical investigation, but at the same time having the same global dynamical behavior of realistic chaotic advection systems. This model has been used in many works to study general properties of chaotic advection [10,17,19].

We consider a system of N particles advected by the flow described by Eq. (1), subject to the gravitational force, to the

drag force due to the fluid's viscosity, and the forces arising from collisions among the particles. Assuming an incompressible fluid, the dimensionless equations of motion are given by [20]

$$\frac{d\mathbf{v}_p}{dt} = -A(\mathbf{v}_p - \mathbf{u}) + \mathbf{G} + \sum_{i \neq p}^N \eta_i \delta(|\mathbf{y}_p - \mathbf{y}_i| - 2r), \quad (2)$$

where $\mathbf{v}_p = \frac{d\mathbf{y}_p}{dt}$ and \mathbf{y}_p are the velocity and position of the particle p , respectively, and \mathbf{y}_i is the position of the particle i which is colliding with particle p . A and \mathbf{G} are the inertia and the gravitation parameters, respectively, and they are given by $A = 9\mu L / 2r^2 \rho_p U$ and $\mathbf{G} = (L/U^2)\mathbf{g}$, where μ is the dynamic viscosity. L and U are, respectively, the typical large-scale length and flow velocity. The quantity η_i is proportional to the momentum transferred to particle p due the collision with the i th particle; it depends on the details of each particular collision, and is determined from the laws of conservation of energy and angular momentum (we assume the collisions are elastic). On the right-hand side of Eq. (2), the first term represents the acceleration associated with the Stokes drag force, the second is the influence of the gravitational field and the third is the collision term. In the limit $A \rightarrow \infty$, one recovers the Hamiltonian system where the particles are ideal tracers and no dissipation is present. In this study we fix $\mathbf{G} = -4\mathbf{j}$, where \mathbf{j} is the unitary vector in the positive direction of the ordinate axis.

To simulate the dynamics of this system, we take into account the fact that the motion of a particle p is due to both continuous forces (drag, advection and gravitation) and discontinuous forces (collisions). In intervals without collisions, the last term in Eq. (2) is zero, and Eq. (2) is a normal differential equation, which can be integrated using the usual methods. Whenever there is a collision between any two particles p and i , the particle positions do not change during the collision (which we regard as instantaneous) and the particle velocities \mathbf{v}_p and \mathbf{v}_i are determined from the conservation of momentum and kinetic energy of the two particles.

The detailed procedure we use to evolve the system in time is as follows. In any given time step, we first integrate numerically Eq. (2) using the fourth-order Runge-Kutta method with a fixed time step Δt (we used $\Delta t = 0.02$), without the collision term. Then, we identify when the first collision occurs (if any) during the time-step interval, by keeping track of the distances between all pairs of particles. A collision occurs if during this interval the distance between the centers of any two particles becomes less than twice the particles' radius. If a collision takes place, we determine the collision time by interpolation, and revert the state and the time of the system back to the collision time. We then calculate the velocities of the colliding particles as explained above. If no collision is detected in the interval Δt , no correction is done. We then go on to the next step, and so on.

III. RESULTS

In order to analyze the collective dynamics of this system, we define the dispersion D of the particles as the average $D(t) = \langle d_i(t) \rangle$, where d_i is the distance between particle i

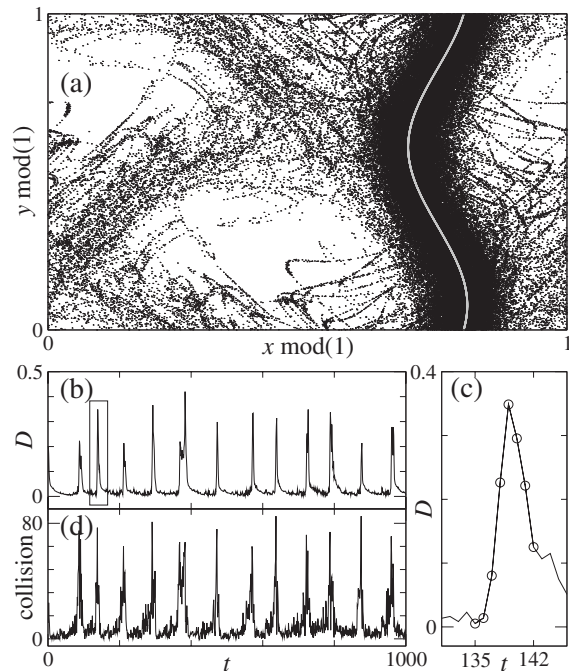


FIG. 1. (a) The gray curve is the collisionless quasiperiodic attractor. Black points are the superposition of the positions of $N=250$ interacting particles for $D>0.02$, plotted at integer times $[t \bmod(1)=0]$. (b) Dispersion D as a function of time. (c) Magnification of the box in (b). The circles represent the dispersion from $t=135$ to 142 relative to particles disposition in Fig. 2. (d) Number of collisions during each time interval $\Delta t=1$. The parameters are $A=3.0$ and $r=0.001$.

$\in [1, N]$ and the closest point on the quasiperiodic attractor. Figure 1(a) shows in black the superposition of successive positions of $N=250$ particles with radius $r=0.001$, taken at stroboscopic times t such that $t \bmod 1=0$ (in other words, for integer values of t), from $t=50$ to $t=10^3$ with $D>0.02$ and $A=3.0$. The gray line depicts the quasiperiodic attractor of the collisionless dynamics. Note that in this interval, the particles are mainly distributed around two regions: the quasiperiodic attractor and, as we will show shortly, a coexisting chaotic saddle. Figure 1(b) shows the evolution of the dispersion D with time. We see that the system displays a pulsed behavior, in which the particles concentrate for a long time around the quasiperiodic attractor before suddenly bursting to spend a short time around the chaotic saddle; after some time there, they return to the vicinity of the quasiperiodic single-particle attractor, and the next cycle starts.

In the beginning of each cycle in this intermittency, the particles converge to the quasiperiodic attractor, and would remain there in the absence of collisions. To understand why they leave the quasiperiodic attractor, we analyze, step by step, their trajectories at the onset of a burst. In Fig. 2, we show in detail how the spatial distribution of $N=250$ particles changes in time during one of the bursts. The particle positions are plotted from $t=135$ to 142.75, at time intervals of 0.25. We see that initially the particles are concentrated around the quasiperiodic attractor, and then they suddenly start diverging from it. They eventually end up near the chaotic saddle to the left of the attractor. The corresponding

spike in the dispersion is indicated in Fig. 1(b) and magnified in Fig. 1(c). We found that in typical bursts a spike takes about $\Delta t=4$ to reach its maximum.

The gray curve on the right of each of the plots in Fig. 2 depicts the quasiperiodic attractor. Observe that its shape changes in time, following the periodic time dependence of the flow. For $t=135$ the particles are practically on the attractor, but they start diverging from it as the number of collisions increases, as shown in the plots for $t=135.25$, 135.5, and 135.75. Note that there are clusters of particles near the sharp corners seen in the plots for $137 \leq t \leq 138.75$. The density of particles is higher at these corners, which causes the number of collisions in these regions to increase, with a consequent increase in the total dissipation in the system and the further accumulation of particles in those regions [27]. As time goes on, this leads to the formation of sharper and sharper corners in the spatial distribution of particles. This accumulation of particles further increases the frequency of collisions, which eventually causes the dynamics to depart dramatically from the collisionless case. The result is that the particles accumulated there suddenly leave the neighborhood of the attractor, and spread out very quickly across the spatial cell. This can be seen in Fig. 2 ($135 \leq t \leq 139$). The particles then eventually distribute themselves in the complicated pattern seen in Fig. 2; this structure shadows the chaotic saddle located to the left of the quasiperiodic attractor. Since the accumulating mechanism operating in the quasiperiodic attractor is not present in the nonattracting, unstable saddle, the collision frequency drops. As a result, the particles follow again roughly the collisionless dynamics, which directs them towards the quasiperiodic attractor. Hence after some time, the particles converge again to the vicinity of the collisionless quasiperiodic attractor, as seen in Fig. 2 from $t=139.25$ to the end. The accumulation process then begins again, and the cycle starts anew.

In order to test the mechanism for the pulsed behavior of the dispersion proposed above, we plot in Fig. 1(d) the number of collisions as a function of time. We see that the collision frequency rises sharply just before each peak in the dispersion, confirming that the bursting episodes are caused by an increase in the number of collisions caused by their accumulation.

We can gain a better understanding of how the underlying collisionless dynamics is related to the full collective dynamics of the interacting particles by focusing on the time τ it takes single particles (without collisions) to reach the quasiperiodic attractor. We call τ the flight time. In Fig. 3 we plot the flight time of the particles shown in Fig. 2 as a function of their initial position $y \bmod(1)$. Figures 3(a)–3(c) show τ of particles at times $t=136$, 137, and 138, respectively; compare with the corresponding plots of Fig. 2. When calculating τ , we consider a particle to have reached the attractor when its distance from it is less than $\delta=0.05$; we obtain essentially the same results for a wide range of δ . Comparing the particles' flight times with their positions in Fig. 2, we note that the highest flight times correspond to the particles which are in the corner regions, where they are most concentrated.

We also determine the collisionless system's bifurcation diagram, shown in Fig. 4(a). For the parameter range from $A=2.5$ to 4, we change the parameter by steps of size ΔA

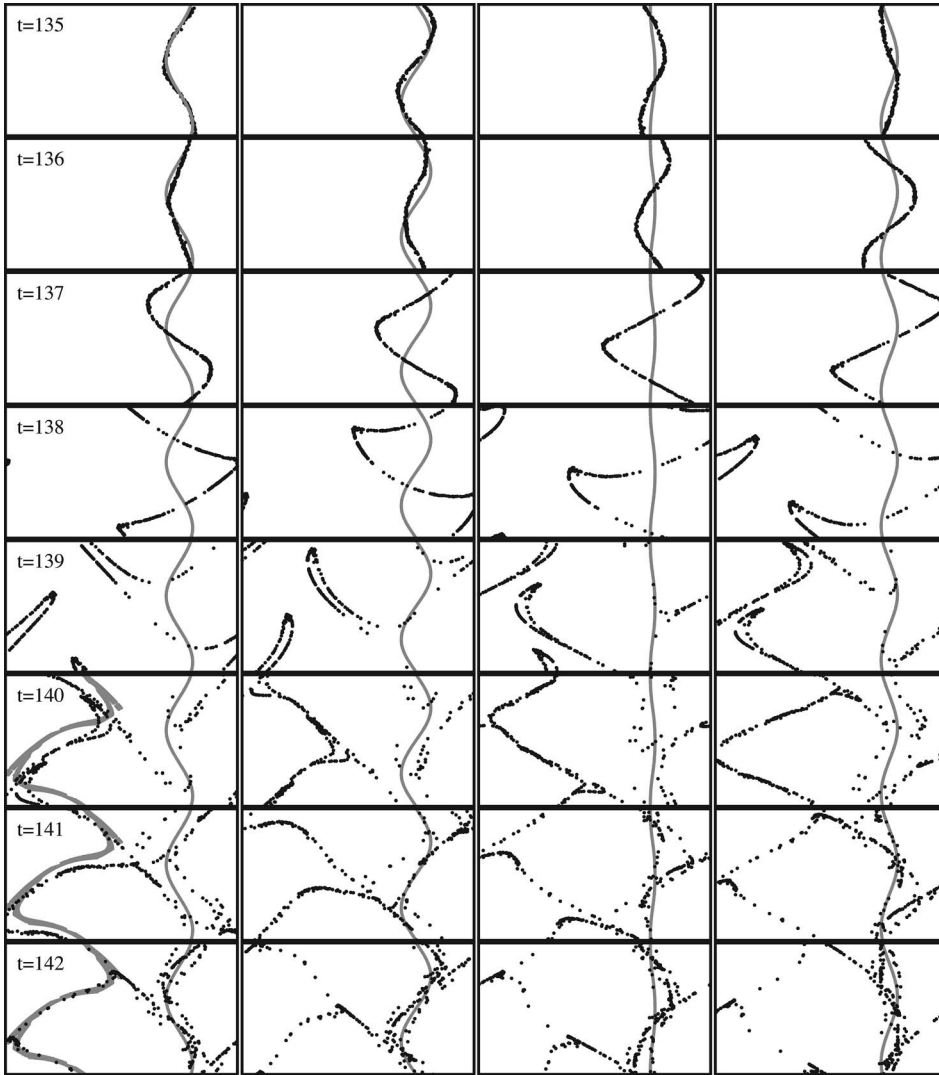


FIG. 2. Time evolution of the positions of 250 particles. Each plot is a snapshot of the positions of the particles at a given time. From the first column to the fourth, $t \bmod(1) = 0, 0.25, 0.5,$ and 0.75 . The integer part of the time is labeled in the first column. So in the first row, from the left to the right we have $t = 135, t = 135.25, t = 135.5,$ and so on. The gray curve on the right side [$x \bmod(1) > 0.5$] of each plot is the collisionless quasiperiodic attractor. For $t = 139, 140, 141,$ and 142 , the gray points on the left side [$x \bmod(1) < 0.5$] are the chaotic saddle for the collisionless dynamics found with the sprinkler method, as discussed in the text. The ordinate and abscissa axis are $y \bmod(1)$ and $x \bmod(1)$, respectively.

$= 0.005$ and, for each parameter value, we evolve 50 collisionless particles with initial positions chosen randomly, and with velocities satisfying $v_x = u_x(y, 0)$ and $v_y = u_y(x, 0)$. We let the transient die out and plot the corresponding x coordinates. For $A = 3.0$, the black region in Fig. 4(a) represents the region in $x \bmod(1)$ where the collisionless quasiperiodic attractor is located. Note that there is also a periodic attractor in the range $x \bmod(1) < 0.5$, for $A \approx 3.5$, and a chaotic attractor for $3.65 \lesssim A \lesssim 3.95$; in both cases it coexists with the quasiperiodic attractor. Figure 4(b) shows both the quasiperiodic and chaotic attractors for $A = 3.7$. The shape of this chaotic attractor of the collisionless dynamics is almost identical to the structure formed in the collisional case, shown in Fig. 1(a), even though the parameters are quite different ($A = 3.0$ for the collisional case). We have verified that before this

region becomes an attractor, there is a chaotic saddle for $A = 3.6$ with practically the same shape as the attractor. To establish the connection between this saddle in the collisionless dynamics and the structure seen in the pulse regime when the collisions are present, we took the particle states of the collision dynamics with $A = 3.0$ at times $t = 136, 137,$ and 138 as initial conditions for the collisionless system with $A = 3.6$, and evolve them neglecting the collisions, as in Fig. 3. The result shows the strong connection between the two situations. In Fig. 5(f) it is seen that many particles reach the left side of the space, describing the characteristically shaped structure with filaments and folds, also discernible in Fig. 2. Particles that visit this structure have long flight times. The large fluctuations in the particles' flight times, shown in Fig. 5(c), reveal an acute sensitivity of the dynamics to initial

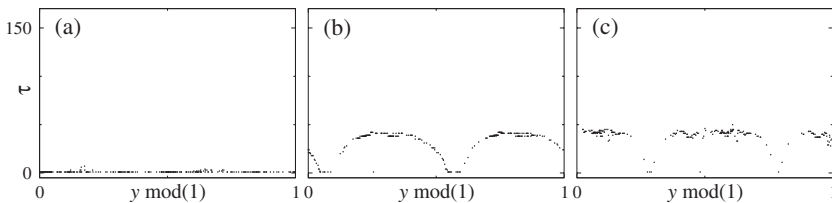


FIG. 3. (a), (b), and (c) are the flight time of particles sets at $t = 136, 137,$ and 138 shown in Fig. 2, respectively. $A = 3.0$.

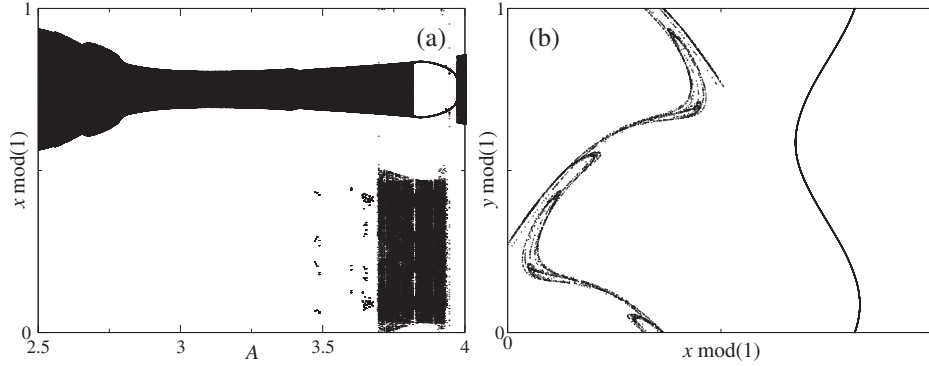


FIG. 4. (a) Bifurcation diagram for the collisionless system given by Eq. (2). (b) Attractors for $A=3.7$. Depending on the initial condition, a particle may converge to the chaotic attractor on the left side or to the quasiperiodic attractor on the right side.

conditions, which is the signature of a chaotic saddle. We conclude that the collisionless dynamics displays transient chaos for $A=3.6$. We note that the chaotic saddle is actually a $4N$ -dimensional structure, since Eq. (2) defines a $4N$ -dimensional dynamical system. We see only its projection onto the “single-particle” x - y plane.

The coexistence of an unstable and a stable set in phase space is commonly associated with the phenomenon of excitability [21,22]. In our case, the stable set is the quasiperiodic attractor of the collisionless dynamics, and the unstable set is the chaotic saddle present in the full collisional dynamics. In excitable systems, the particles all eventually converge to the attractor, but they do so by two very different routes. If a particle is close to the attractor (in its basin of attraction), it converges to it very quickly. If, however, a particle is initially at some distance from the attractor, and is close to the stable manifold of the unstable set, it approaches the attractor only after a long excursion; it initially moves along the stable manifold of the unstable set (in our case, the chaotic saddle), stays near the saddle for possibly long times, and then goes back to the neighborhood of the collisionless quasiperiodic attractor. This is very close to the behavior we observe in our multiparticle system. The difference is that the

quasi-periodic attractor is only an attractor in the absence of collisions; collisions cause the particles to eventually spread out and reach the vicinity of the saddle’s stable manifold, as we have seen. This excitable behavior can be seen in Fig. 5: as collisions make the particles spread out away from the quasiperiodic attractor, at around $t=137$, many particles reach the saddle’s stable manifold, and they visit the chaotic saddle region, taking a large excursion before returning to the stable set.

We use the sprinkler method [23,24] to visualize the chaotic saddle of the collisionless dynamics, with 10^6 initial conditions. The saddle structure is shown on the left side of Fig. 2 with $t=139, 140, 141,$ and 142 . This sequence shows that even when the chaotic saddle is not observed for the single particle dynamics, the interaction between particles effectively creates a chaotic saddle which shadows the saddle present in the single-particle case for a different range of parameters.

IV. DISCUSSION AND CONCLUSIONS

Behavior in some respects similar to what we report here has been observed in single-particle systems acted on by random noise [25]; in particular, the appearance of a chaotic saddle due to collisions is analogous to the appearance in some systems of a saddle caused by noise, as described in Ref. [26]. However, we have verified that the instability reported in Ref. [25] cannot be generated by noise alone: the interaction between particles is crucial for this phenomenon to occur. In systems where an attractor coexists with a chaotic saddle, particles quickly approach the saddle and leave it along the unstable direction. Noise-induced chaos in such systems populates the unstable manifold of the saddle [26]. We have simulated the single-particle dynamics in our system, and we do not observe this behavior: when acted on by noise and in the absence of interactions, the particles stay near the quasiperiodic attractor, and do not display the striking periodic bursts observed in the presence of collisions. This difference between the one-particle noisy dynamics and the collisional system is that, in the latter case, the perturbation in the motion of a given particle caused by its collision with another particle is determined by the direction of the flow. In the random noise case, on the other hand, the perturbation can be in all directions with the same probability. Furthermore, the frequency of collisions increases with the density of particles, which introduces yet another effect not

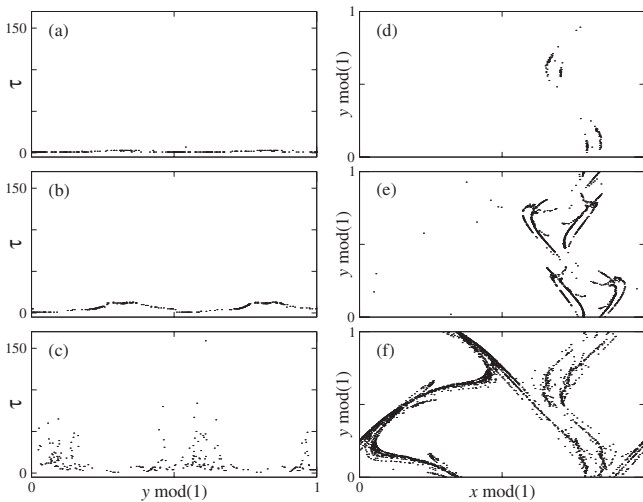


FIG. 5. For $A=3.6$, in (a), (b), and (c) are the flight time of particles sets at $t=136, 137,$ and 138 shown in Fig. 2, respectively. (d), (e), and (f) are the corresponding trajectories, plotted at integer times, until each particle reaches the vicinity of the quasiperiodic attractor.

present in purely random noise. This means that the effects of the interparticle interactions cannot be reduced purely to noise, because there are important correlations present in the multiple-particle dynamics which are absent in the corresponding single-particle noisy model. In making the above comparison with one-particle noisy systems, we only considered the simplest kind of noise, namely, additive uncorrelated noise. In view of the dependency of collision frequency with particle density, it would be interesting to compare our results considering collisions with those obtained with more complex kinds of noise, such as multiplicative noise with a strength that depends on the local number of particles.

In conclusion, we investigated the dynamics of systems of colliding particles advected by chaotic flows, and found that the interaction between particles gives rise to very unexpected collective phenomena not found in the noninteracting case. The most striking collective behavior is the occurrence

of periodic burstings in the spatial distribution of the particles, in which they venture far away from the single-particle quasiperiodic attractor. We have explained this phenomenon in terms of a chaotic saddle present in the dynamics. We have also compared this collective behavior with that of a single-particle system influenced by noise, and concluded that the dynamics we observe cannot be explained purely in terms of noise: the correlation of the particle motion is crucial for generating this behavior. This shows that this is really a collective phenomenon, which is determined by the global dynamics of the system.

ACKNOWLEDGMENTS

We thank the financial support of FAPESP, CNPq, OTKA Grant No. T72037, MRC Grant No. G0502236, and the College of Physical Sciences, University of Aberdeen.

-
- [1] Z. Toroczkai, G. Károlyi, A. Péntek, T. Tél, and C. Grebogi, *Phys. Rev. Lett.* **80**, 500 (1998).
- [2] G. Metcalfe and J. M. Ottino, *Phys. Rev. Lett.* **72**, 2875 (1994).
- [3] I. R. Epstein, *Nature (London)* **374**, 321 (1995).
- [4] E. R. Abraham, *Nature (London)* **391**, 577 (1998).
- [5] A. Bracco, A. Provenzale, and I. Scheuring, *Proc. R. Soc. London, Ser. B* **276**, 1795 (2000).
- [6] I. Scheuring, G. Károlyi, A. Péntek, T. Tél, and Z. Toroczkai, *Freshwater Biol.* **45**, 123 (2000).
- [7] T. Tél, A. P. S. de Moura, C. Grebogi, and G. Károlyi, *Phys. Rep.* **413**, 91 (2005).
- [8] O. Piro and M. Feingold, *Phys. Rev. Lett.* **61**, 1799 (1988).
- [9] T. Nishikawa, Z. Toroczkai, and C. Grebogi, *Phys. Rev. Lett.* **87**, 038301 (2001).
- [10] R. D. Vilela, T. Tél, A. P. S. de Moura, and C. Grebogi, *Phys. Rev. E* **75**, 065203(R) (2007).
- [11] I. J. Benczik, Z. Toroczkai, and T. Tél, *Phys. Rev. Lett.* **89**, 164501 (2002).
- [12] R. D. Vilela and A. E. Motter, *Phys. Rev. Lett.* **99**, 264101 (2007); A. Trabesinger, *Nat. Phys.* **4**, 15 (2008).
- [13] Y. Do and Y.-C. Lai, *Phys. Rev. Lett.* **91**, 224101 (2003).
- [14] J. K. Eaton and J. R. Fessler, *Int. J. Multiphase Flow* **20**, 169 (1994).
- [15] S. Sundaram and L. R. Collins, *J. Fluid Mech.* **379**, 105 (1999).
- [16] W. C. Reade and L. R. Collins, *Phys. Fluids* **12**, 2530 (2000).
- [17] C. López and A. Puglisi, *Phys. Rev. E* **67**, 041302 (2003).
- [18] M. Liu, F.-J. Muzzio, and R. L. Peskin, *Chaos, Solitons Fractals* **4**, 869 (1994); R. T. Pierrehumbert, *ibid.* **4**, 1091 (1994).
- [19] Z. Neufeld, P. H. Haynes, and G. Picard, *Phys. Fluids* **12**, 2506 (2000); Z. Neufeld, C. López, E. Hernández-García, and O. Piro, *Chaos* **12**, 426 (2002).
- [20] M. Maxey and J. Riley, *Phys. Fluids* **26**, 883 (1983).
- [21] E. Izhikevich, *Int. J. Bifurcation Chaos Appl. Sci. Eng.* **10**, 1171 (2000).
- [22] D. Gomila, M. A. Matías, and P. Colet, *Phys. Rev. Lett.* **94**, 063905 (2005).
- [23] H. Kantz and P. Grassberger, *Physica D* **17**, 75 (1985).
- [24] G. H. Hsu, E. Ott, and C. Grebogi, *Phys. Lett. A* **127**, 199 (2004).
- [25] G. Károlyi, T. Tél, A. P. S. de Moura, and C. Grebogi, *Phys. Rev. Lett.* **92**, 174101 (2004).
- [26] L. Billings and I. B. Schwartz, *J. Math. Biol.* **44**, 31 (2002).
- [27] This increase in dissipation occurs despite the fact that the collisions are elastic. The reason is that after a collision, the velocity of the particles are altered, generating a sudden and intense velocity difference between the particle and the surrounding flow, which by Eq. (2) means an increase in the dissipative Stokes force.